Non-close packaged monolayer of silica nanoparticles on silicon substrate using HF vapour etching

Nguyen Van Minh[1], *Nguyen Ngoc Son*[1], *Nghiem Thi Ha Lien*[2], *Chu Manh Hoang*[1] ✉

[1]*International Training Institute for Materials Science, Hanoi University of Science and Technology, Hanoi, Vietnam*
[2]*Institute of Physics, Vietnam Academy of Science and Technology, 18 Hoang Quoc Viet, Cau Giay, Ha Noi, Vietnam*
✉ *E-mail: hoangcm@itims.edu.vn*

Published in Micro & Nano Letters; Received on 12th January 2017; Revised on 31st March 2017; Accepted on 11th April 2017

Ordered monolayer of silica nanoparticles assembled on solid substrates is useful for a variety of promising applications in photonics, plasmonics, and solar cell. Nanoparticles are usually assembled into close- or non-close-packed monolayer (CPM) form. The non-close packed monolayer can be directly deposited from mono-dispersed colloidal suspension onto a solid substrate in terms of using complicated techniques or tuning the size of nanoparticles in the CPM. An effective method for forming the non-close packed monolayer of silica nanoparticles is reported. Silica nanoparticles are self-assembled into the CPM on silicon substrate. The size of silica nanoparticles is tuned by high frequency vapour etching. The dependence of the size and shape of silica nanoparticles on etching time is presented. The effect of sintering conditions on the etching process is also investigated.

1. Introduction: Non-close packed monolayer (NCPM) of nanoparticles on solid substrates has various applications such as in photonics, surface enhanced Raman scattering, and solar cell [1–3]. There are several methods introduced for fabricating NCPMs, which can be classified into direct and indirect approaches. In the former approach, the NCPM is realised by one-step technique such as freeze drying method [4], template directed assembly [5], and quartz crystal piezoelectric oscillation [6]. This approach requires complicated machines and experimental accessories. In the indirect approach, close-packed monolayer (CPM) is first fabricated, following by reducing the size of all particles by plasma etching [7] or reactive ion etching [8] to create the NCPM. The NCPM can also be formed by tuning the gap between particles by substrate elongation while maintaining the size of particles [9]. In addition, the spin coating of colloidal particles with polymeric additives [10] or the use of optical tweezers [10] can also be utilised for fabricating NCPMs. Tuning the size of particles in the CPM is useful achievement for various applications, for example, in fabricating plasmonic nanostructures and solar cell [3, 11–14].

In this Letter, the NCPM is fabricated by reducing the size of silica nanoparticles in an assembled CPM. Silica nanoparticles with a mean size of around 50 nm are synthesised by sol–gel method. Silica nanoparticles are used instead of nanoparticles made of other materials because silica is a common material in nanotechnology. Tuning the size of silica nanoparticles in the CPM to form the NCPM is carried out by high frequency vapour etching. Using this method we can tune the size of silica nanoparticles at nano scale. The initial CPM is created by the drop-coating method on a slanted substrate with the assistance of infrared irradiation in the solvent evaporation process. The dependence of size and shape of silica nanoparticles on etching time is investigated. In addition, the effect of sintering conditions on the etching process is also presented.

2. Experimental process

2.1. Preparation of close-packed silica nanoparticle monolayer: A 4-inch, type-p Si(100) wafer is cut into 1 cm × 1.5 cm substrates, which are cleaned and rendered to hydrophilic by appropriate techniques as follows. Firstly, the Si substrates are sequentially ultra-sonicated in acetone, ethanol, and deionised (DI) water to clean dust particles and organic substances from the substrate surface. The Si substrate wettability is crucially important for the self-assembling process of nanoparticles into the CPM. Hence, the Si substrates are then processed by next two steps. The cleaned Si substrates are immersed into the oxidising solution containing a mixture of H_2SO_4 and H_2O_2 (H_2SO_4(97%): H_2O_2(35%) (3 : 1 (v/v))) for 18 h. Their surfaces are changed into hydrophilic by immersing the substrates into the solution H_2O:NH_4OH:(30%)H_2O_2 (5 : 1:1 (v/v/v)) for 20 min. at the 80°C processing temperature. In this step, the SiO_2 surface formed in the oxidising process is terminated with silanol (≡Si-OH) groups, which are active for the chemical and physical absorption of water molecules. After each step, the Si substrates are washed with the DI water flow. Finally, they are kept in the DI water prior to use.

A colloidal suspension with silica nanoparticles dispersed in ethanol with wt% of 0.25%, was prepared by sol–gel method. This process can be described as follows. A 2.8 ml volume of ammonium hydroxide (NH_4OH, 29% in water) was added to 30 ml ethanol under vigorous stirring for 30 min. The silica nanoparticles suspension solution was then formed by adding 300 µl tetraethylorthosilicate (TEOS, 99%) under continuous stirring [15]. To achieve the desired size of silica nanoparticles, the sol–gel process has been modified compared with that reported in literature [16–18]. In the sol–gel process, we used TEOS with low concentration (0.045 M) and carried out at room temperature. The size of silica nanoparticles is controlled by verifying the amount of NH_4OH, which increases with the added amount of NH_4OH without adding water. Prior to coating on the Si substrate, the colloidal suspension was ultra-sonicated in 10 min. to disperse particles evenly and mixed with the DI water. The colloidal suspension is mixed with the DI water in a volume ratio of 1 : 1 that is the optimal ratio to obtain large monolayer area.

To form the CPM, we employed the drop-coating technique on tilted Si substrate with the assistance of infrared irradiation during the solvent evaporation process. Here, we employed the tilted substrate method to assemble the CPM with the large monolayer area [19]. The optimal angle for the tilted substrate for assembling the CPM with the size of silica nanoparticle used in our present research is 30°. Schematic of the drop-coating experiment process is shown in Fig. 1. A droplet of colloidal solution is dropped onto the tilted Si substrate. Due to high degree of substrate wettability, the droplet is quickly spread over the substrate surface.

doi: 10.1049/mnl.2016.0825

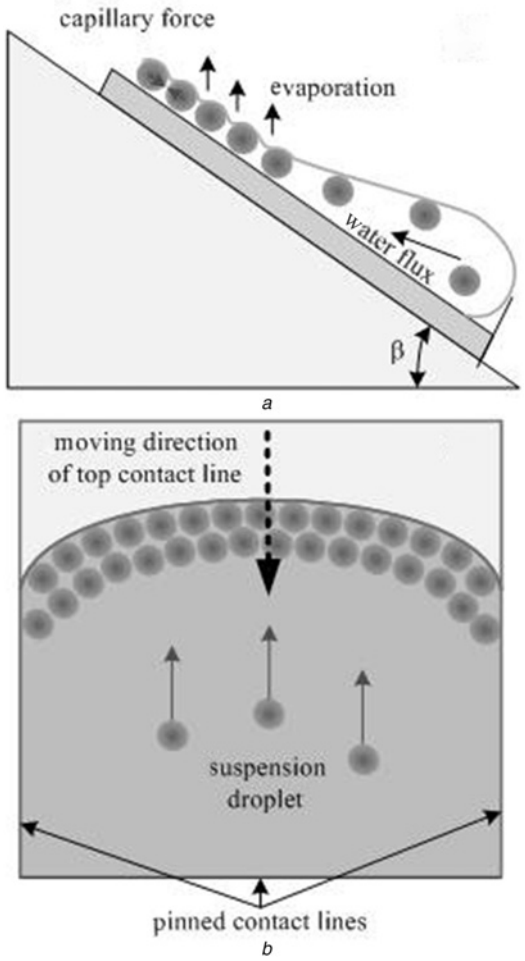

Fig. 1 *Schematic of the drop-coating experiment process*
a Schematic of the drop-coating technique
b Orthogonal view of contact lines of a spread solution droplet on the Si substrate showing the moving direction of top contact line; other contact lines are pined at edges of the Si substrate

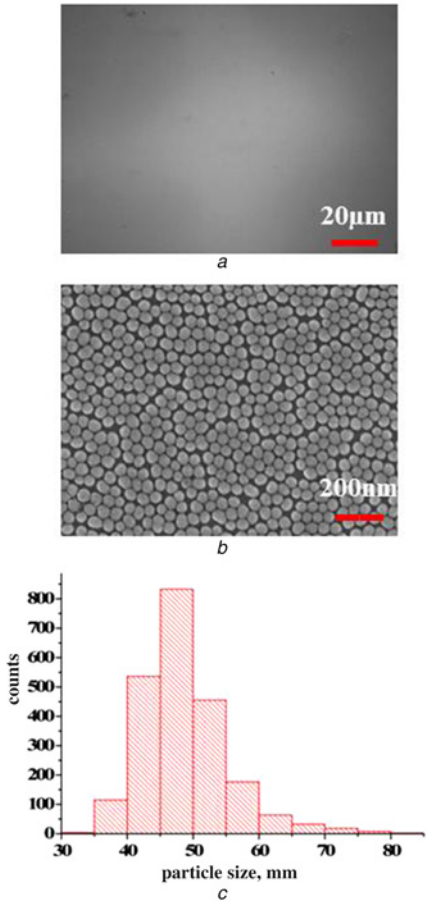

Fig. 2 *CPM with optimised self-assembly process*
a FESEM image of a continuous CPM
b Magnification image of a CPM region
c Distribution of silica nanoparticle size
All the FESEM images were measured under the electric field of 5 kV

The CPM is governed by the attractive capillary force between silica nanoparticles and moving speed of the top contact line. After the drying process, the Si substrate with coated silica nanoparticles is annealed at 100°C in 15 min. to evaporate residual solvent.

The CPM with optimised self-assembly process is shown in Fig. 2. Figs. 2*a* and *b* shows field emission scanning electron microscopic (FESEM) image of a continuous CPM and magnified FESEM image of a CPM region, respectively. The distribution of silica nanoparticle size is shown in Fig. 2*c*. The continuous monolayer area is on the scale of some square millimetres. The average size of silica nanoparticles is 50 nm.

2.2. Fabrication of non-close packed silica nanoparticle monolayer: After the successful deposition of the CPM, the Si substrate with the CPM is firstly sintered at 900°C for 60 min. After cooling down, the sintered CPM is subjected to a HF vapour system to reduce the size of silica nanoparticles. After this step, the Si substrate with the CPM is sintered in step 2, at a temperature of 1100°C for 30 min. and put into the HF vapour system again for reducing further the size of silica nanoparticles. The HF vapour system is operated at room temperature (25°C). The sample is put at the center of a HF chamber made of Teflon which is ~2 cm from the HF49% solution surface. In our experiment, the sample is not in contact directly with the HF vapour flow. The HF vapour flows from the backside of the substrate to the frontside. This setup is to reduce etching rate of silica nanoparticles in the HF49% vapour, which is easier for controlling manually the etching process. The etching stop is realised by opening the cover of the HF chamber after a desired etching time. When the cover is opened, an air intake system is used for exhausting HF vapour. Thus, the sample is not affected by HF vapour anymore.

3. Results and discussion: To tune the gap between silica nanoparticles, the Si substrate with the CPM is etched in HF vapour. FESEM images of the CPM after etched in 7 and 10 s are shown in Figs. 3*a* and *b*, respectively. The results indicate that direct etching in HF vapour is insufficient for reducing the size of silica nanoparticles. After the etching time of 7 s, the size of silica nanoparticle is almost unchanged and quickly reduced to zero with the etching time of 10 s. This unwanted result can be explained by the high porosity of silica nanoparticles prepared by sol–gel method from TEOS. In nature, silica nanoparticles synthesised from sol–gel process has the porosity characterisation, which shows low density. This can be confirmed by weighting dry silica nanoparticles [16–18]. HF molecules move inside the silica nanoparticles and react with SiO_2. Fig. 3*b* shows the aggregation of chemical reaction products created from the etching process into new particles, in which their size ranges from 100 to 200 nm. These new particles are separated on micrometre scale. The reaction between SiO_2 and HF produces fundamentally SiF_4 and H_2O in the form of gas left the substrate. This is true for dry HF gas and at high temperature. The reaction equations between SiO_2 and HF are shown in (1) and (2). In fact,

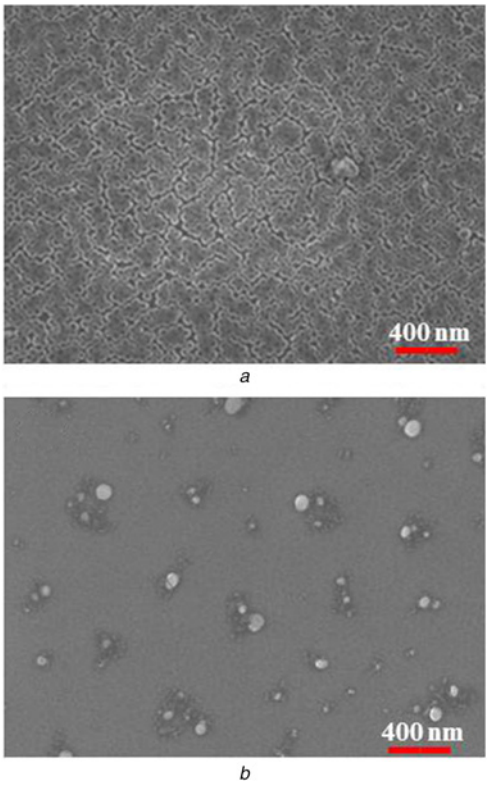

Fig. 3 *FESEM images of the CPM after etched in HF Vapour*
a 7 s
b 10 s

the HF vapour is produced from aqueous HF 49%. So, the etching agent is HF/H_2O. It is pointed out in [20] that this etching agent creates last product H_2SiO_3 in the form of complex molecular particles. The equation for this reaction is shown in (3).

$$SiO_2 + 6HF \rightleftarrows H_2SiF_6 + H_2O \quad (1)$$

$$H_2SiF_6 \rightleftarrows SiF_4 + 2HF \quad (2)$$

$$H_2SiF + 3H_2O \rightleftarrows H_2SiO_3 + 6HF \quad (3)$$

Moreover, larger particles created after etching may be due to high humidity, which leads to the formation of H_2SiO_3 as shown in (3). These are nuclear for creating particles with larger size than that of initial silica nanoparticles.

The porosity of silica nanoparticles can be resolved by sintering the CPM substrate. Before the HF vapour etching, the CPM substrate is sintered in a furnace at 900°C for 60 min. After sintering, the size of silica nanoparticle is almost unchanged, as shown in Fig. 4*a*. The HF vapour etching is then carried out with etching times of 20, 40, and 60 s. The FESEM images for each etching time are shown in Figs. 4*b–d*, respectively. Figs. 4*e* and *f* show the distribution of silica nanoparticle size after etched for 20 and 40 s, respectively. The FESEM images indicate that, the size of silica nanoparticle is smaller as etching time increases. However, in the last case with the etching time of 60 s, nanoparticles begin to fall down due to broken linking necks resulting from the HF vapour etching process, as shown in Fig. 5.

To resolve the problem of fallen-down nanoparticles, after etching in 40 s, the NCPM substrate is sintered at 1100°C for 30 min. to shrink down nanoparticles and proceeds in HF vapour for 20 s. The FESEM image of NCPM after the second step sintering and etching is shown in Fig. 6*a*. Fig. 6*b* shows the magnification of a NCPM region. The result indicates that only a few

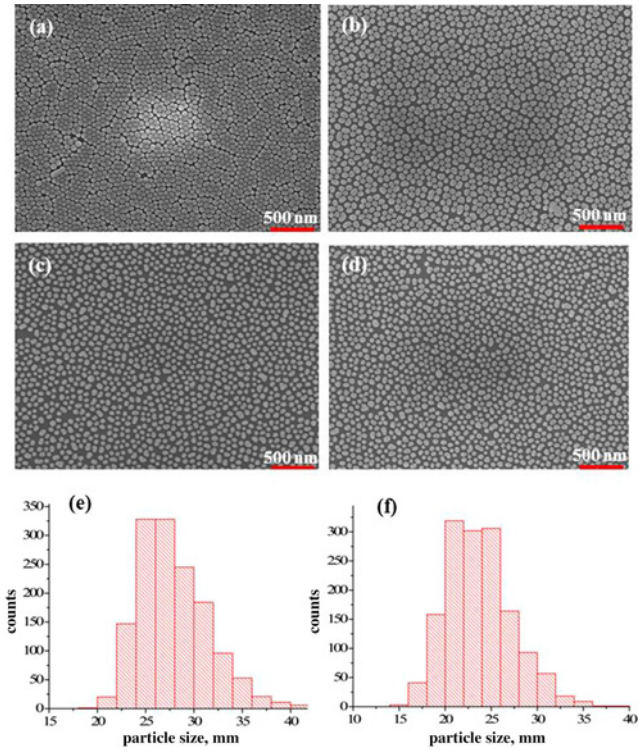

Fig. 4 *FESEM images of the CPM*
a After sintered
b After etched by HF vapour for 20 s
c After etched by HF vapour for 40 s
d After etched by HF vapour for 60 s
e and *f* Distribution of silica nanoparticle size after etched for 20 and 40 s

nanoparticles are fallen down. This can be caused by non-uniform of silica nanoparticles synthesised by sol–gel method. However, the result shows that we can tune the size of silica nanoparticles. Fig. 6*c* shows the distribution of nanoparticle size after etching. Fig. 6*d* shows the dependence of average nanoparticle size on etching time for each sintering step. The result shows that we can tune the size of silica nanoparticles from 50 to 20 nm. The further reduction can obtain by optimising the sintering temperature and etching time. It proves that the sintering parameters in step 2 are effective in shrinking silica nanoparticles. The height change of nanoparticle after HF vapour etching is not investigated. However, silica nanoparticles are considered to be spheres. After etching without

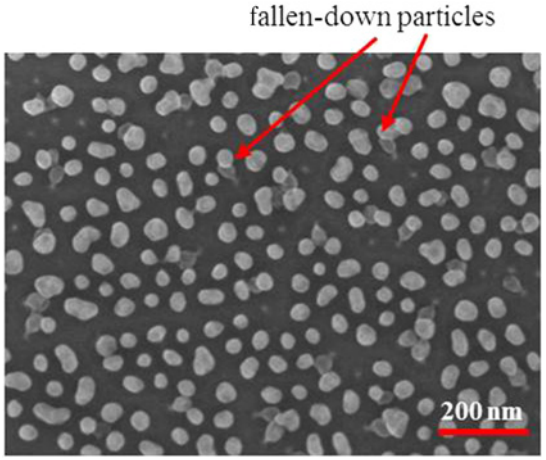

Fig. 5 *FESEM image shows silica nanoparticles etched by HF vapour, which are fallen down due to broken linking necks*

doi: 10.1049/mnl.2016.0825

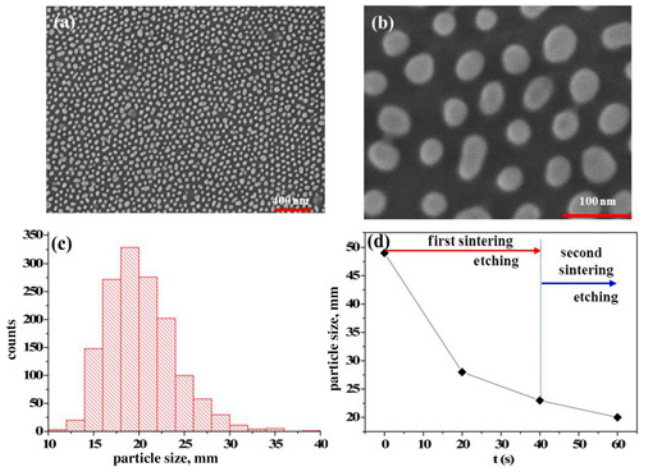

Fig. 6 *FESEM images*
a NCPM after the second step sintering and HF vapour etching in 20 s
b Magnification image of a NCPM region
c Distribution of silica nanoparticle size
d Dependence of the average nanoparticle size on etching time for each sintering step

annealing, silica nanoparticles might be changed into prolate spheroids due to isotropic etching property of HF vapour. After annealing, prolate spheroids are transformed into prolate semi-spheroidal shapes. In general, the height change of nanoparticle after HF vapour etching depends on etching time and annealing process. The gap between silica nanoparticles can be measured via top-view SEM images of the samples before and after etching. Before etching, the silica nanoparticles is assembled into the closed-packaged monolayer. Some region seen in SEM images, there exists gap between silica nnanoparticles. This is caused by the non-perfect uniform of the synthesised silica nnano-particles. However, due to the nature of the closed-packaged mono-layer we can consider the gap between silica nnanoparticles before etching to be zero. After etching, we determine the gap between silica nanoparticles by the difference of average particle size and the distance between the centre of the particles. For instance, after etching step 2 for 20 s the average size of silica nanoparticles are 20 nm. The gap between silica nanoparticles is derived to be 80 nm when the initial silica nanoparticles with the size of 50 nm assembled into the CPM. In general, the proposed method can be used for patterning the silica particles at any size. However, we used 50 nm silica nanoparticles as a mask to create sub-50 nm silicon nanostructures after etching silicon substrate. Such silicon nanostructures may have some emerging optical properties when quantum effect appears. This very fine tuning method allows to fabricate array of nanostructures using the NCPM as a mask for etching [11, 12]. Furthermore, the fine tuning of gap between nano-particles is potential for plasmonic substrates [13, 14].

4. Conclusion: We have successfully fabricated the NCPM of silica nanoparticles on Si substrate. The NCPM is formed by tuning the size of the silica nanoparticles in the close packed monolayer by HF vapour etching. To tune the size of silica nanoparticles, two-step sintering process is employed. Using this process, we can reduce the size of silica nanoparticles from 50 to 20 nm. This process is simple and cost-effective, which is useful for applications in fabricating plasmonic elements and solar cell.

5. Acknowledgments: This research is funded by HUST Basic Research Foundation for Science and Technology Development under grant no. 'T2015-243'.

6 References

[1] Cai Z., Liu Y.J., Leong E.S.P., *ET AL.*: 'Highly ordered and gap controllable two-dimensional non-close-packed colloidal crystals and plasmonic–photonic crystals with enhanced optical transmission', *J. Mater. Chem.*, 2012, **22**, pp. 24668–24675
[2] Jing J., Yuqin Z., Gangqiang D.: 'The infrared transmission through gold films on ordered two-dimensional non-closepacked colloidal crystals', *J. Semicond.*, 2014, **35**, (9), 092001 (5pp)
[3] Garnett E., Yang P.: 'Light trapping in silicon nanowire solar cells', *Nano Lett.*, 2010, **10**, (3), pp. 1082–1087
[4] Feng C., Choi H.W.: 'Density-tunable non–close-packed monolayer of silica nanospheres prepared by single-step freeze-drying', *J. Vac. Sci. Technol. B*, 2014, **32**, 051805 (5pp)
[5] Yin Y., Lu Y., Gates B., *ET AL.*: 'Template-assisted self-assembly: A practical route to complex aggregates of monodispersed colloids with well-defined sizes, shapes, and structures', *J. Am. Chem. Soc.*, 2001, **123**, pp. 8718–8729
[6] Schmudde M., Grunewald C., Goroncy C., *ET AL.*: 'Controlling the interaction and non-close-packed arrangement of nanoparticles on large areas', *ACS Nano*, 2016, **10**, (3), pp. 3525–3535
[7] Vogel N., Goerres S., Landfester K., *ET AL.*: 'A convenient method to produce close- and non-close-packed monolayers using direct assembly at the air–water interface and subsequent plasma-induced size reduction', *Macromol. Chem. Phys.*, 2011, **212**, pp. 1719–1734
[8] Choi D.-G., Yu H.K., Jang S.G., *ET AL.*: 'Colloidal lithographic nanopatterning via reactive ion etching', *J. Am. Chem. Soc.*, 2004, **126**, pp. 7019–7025
[9] Yan X., Yao J., Lu G., *ET AL.*: 'Fabrication of non-close-packed arrays of colloidal spheres by soft lithography', *J. Am. Chem. Soc.*, 2005, **127**, pp. 7688–7689
[10] Jiang P., Prasad T., McFarland M. J., Colvin V. L.: 'Two-dimensional nonclose-packed colloidal crystals formed by spincoating', *Appl. Phys. Lett.*, 2006, **89**, 11908 (3pp)
[11] Choi J.-Y., Alford T.L., Honsberg C.B.: 'Fabrication of periodic silicon nanopillars in a two-dimensional hexagonal array with enhanced control on structural dimension and period', *Langmuir*, 2015, **31**, (13), pp. 4018–4023
[12] Pudasaini P.R., Ruiz-Zepeda F., Sharma M., *ET AL.*: 'High efficiency hybrid silicon nanopillar–polymer solar cells', *ACS Appl. Mater. Interfaces*, 2013, **5**, (19), pp. 9620–9627
[13] Lei D.Y., Fernández-Domínguez A.I., Sonnefraud Y., *ET AL.*: 'Revealing plasmonic gap modes in particle-on-film systems using dark-field spectroscopy', *ACS Nano*, 2012, **6**, (2), pp. 1380–1386
[14] Lumdee C., Yun B., Kik P.G.: 'Gap-plasmon enhanced gold nanoparticle photoluminescence', *ACS Photonics*, 2014, **1**, (11), pp. 1224–1230
[15] Nghiem T.H.L., Le T.N., Do T.H., *ET AL.*: 'Preparation and characterization of silica–gold core–shell nanoparticles', *Nanopart Res.*, 2013, **15**, 2091 (9pp)
[16] Korzeniowska B., Nooney R., Wencel D., *ET AL.*: 'Silica nanoparticles for cell imaging and intracellular sensing', *Nanotechnology*, 2013, **24**, 442002 (20pp)
[17] Stober W., Fink A., Bohn E.: 'Controlled growth of monodisperse silica spheres in the micron size range', *J. Colloid Interface Sci.*, 1968, **26**, pp. 62–69
[18] Bogush G.H., Tracy M.A., Zukoski IV C.F.: 'Preparation of monodisperse silica particles: control of size and mass fraction', *J. Non-Cryst. Solids*, 1988, **104**, (1), pp. 95–106
[19] Im S.H., Kim M.H., Park O.O.: 'Thickness control of colloidal crystals with a substrate dipped at a tilted angle into a colloidal suspension', *Chem. Mater.*, 2003, **15**, pp. 1797–1802
[20] Hull R.: 'Properties of crystalline silicon' (the Institution of Electrical Engineers, 1999), Technology and Engineering, p. 232, ISBN-13: 978-0863415562